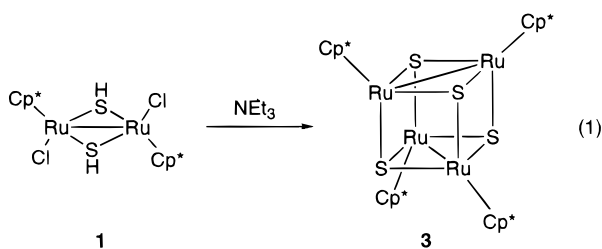


the tri- and tetranuclear sulfido clusters containing the $\text{Cp}^*\text{M}(\mu\text{-S})_2\text{MCp}^*$ fragment. Generation of intermediary $[\text{Cp}^*\text{Ir}(\mu_2\text{-S})_2\text{IrCp}^*]$ from **2a** with the aid of triethylamine has been substantiated from the ^1H NMR study, which finally gives rise to the formation of the cubane-type cluster $[(\text{Cp}^*\text{Ir})_4(\mu_3\text{-S})_4]$. We have now investigated in detail the reactivity of such sulfido-bridged dinuclear species obtained through dehydrohalogenation of the hydrosulfido-bridged dinuclear complexes. In this paper, we describe the trapping of the intermediate $[\text{Cp}^*\text{Ru}(\mu_2\text{-S})_2\text{RuCp}^*]$ with alkynes, which results in the formation of the dithiolene-bridged diruthenium complexes $[(\text{Cp}^*\text{Ru})_2(\mu_2\text{-}\eta^2\text{-}\eta^4\text{-S}_2\text{C}_2\text{R}_2)]$ (**4**). Utilization of **1** as a building block for synthesis of the tri- and tetra-ruthenium sulfido clusters $[(\text{Cp}^*\text{Ru})_4(\mu_3\text{-S})_4]$ (**3**) and $[(\text{Cp}^*\text{Ru})_2(\mu_3\text{-S})_2(\mu_2\text{-H})\text{RuCl}(\text{PPh}_3)_2]$ (**6**) is also reported.

Results and Discussion

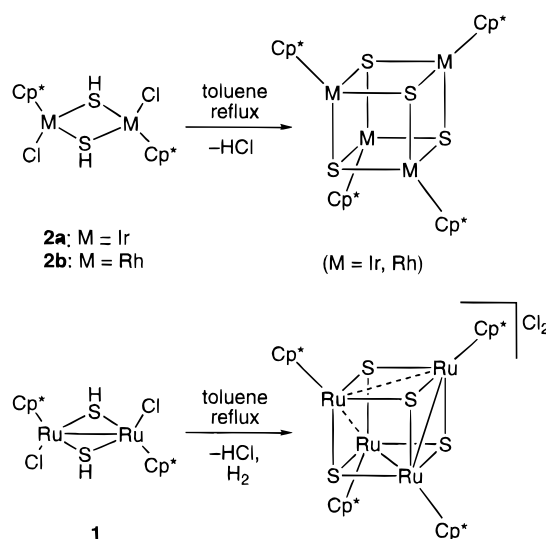
Formation of a Cubane-Type Tetra-ruthenium Sulfido Cluster from a Hydrosulfido-Bridged Diruthenium Complex. We have already demonstrated that the thermolysis of the hydrosulfido-bridged diruthenium complex **1** results in the formation of the dicationic cubane-type cluster $[(\text{Cp}^*\text{Ru})_4(\mu_3\text{-S})_4]\text{Cl}_2$,¹⁰ whereas treatment of the corresponding iridium and rhodium complexes **2** with triethylamine at room temperature affords the neutral cubane-type clusters $[(\text{Cp}^*\text{M})_4(\mu_3\text{-S})_4]$ ($\text{M} = \text{Ir}, \text{Rh}$).¹¹ To clarify the difference between **1** and **2** in the formation of these cubane-type clusters, we have investigated these reactions in more detail.

Like its iridium and rhodium analogues **2**, complex **1** cleanly reacted with an excess of triethylamine to afford the neutral cubane-type cluster $[(\text{Cp}^*\text{Ru})_4(\mu_3\text{-S})_4]$ (**3**) in moderate yield (eq 1). In contrast to the iridium



complex **2a**, however, the intermediary $[\text{Cp}^*\text{Ru}(\mu_2\text{-S})_2\text{RuCp}^*]$ could not be detected by ^1H NMR since the reaction proceeded so fast, similar to that of the rhodium complex **2b**. Facile dimerization suggests a high reactivity of these sulfido-bridged species. It is of interest

Scheme 2



that the platinum analogue $[\text{Pt}(\text{PPh}_3)_2(\mu_2\text{-S})_2\text{Pt}(\text{PPh}_3)_2]$ ¹² and the oxo-bridged complex $[\text{Cp}^*\text{Ir}(\mu_2\text{-O})_2\text{IrCp}^*]$ ¹³ are isolable and do not dimerize, although the former readily reacts with a variety of transition-metal complexes to afford homo- and heterometallic sulfido aggregates.¹² As another related reaction, the hydroxo-bridged diplatinum complex $[\text{Pt}(\text{PMe}_2\text{Ph})_2(\mu_2\text{-OH})_2\text{Pt}(\text{PMe}_2\text{Ph})_2][\text{BF}_4]_2$ is known to be deprotonated with base, giving the corresponding oxo-bridged complex $[\text{Pt}(\text{PMe}_2\text{Ph})_2(\mu_2\text{-O})_2\text{Pt}(\text{PMe}_2\text{Ph})_2]$, which is unstable in solution and converted to the triplatinum oxo cluster $[\{\text{Pt}(\text{PMe}_2\text{Ph})_2\}_3(\mu_3\text{-O})_2][\text{BF}_4]_2$.^{4a} We note that cluster **3** has already been prepared by treatment of $[(\text{Cp}^*\text{Ru})_4(\mu_3\text{-Cl})_4]$ with NaSH, although it requires more forcing conditions and is accompanied by intermittent contamination of $[\text{Cp}^*_4\text{Ru}_4\text{S}_5]$.¹³

On the other hand, when a solution of the iridium and rhodium complexes **2** in toluene was heated under reflux, only dehydrohalogenation occurred to give the neutral cubane-type clusters $[(\text{Cp}^*\text{M})_4(\mu_3\text{-S})_4]$ ($\text{M} = \text{Ir}, \text{Rh}$); H_2 gas was not detected in the reaction mixture (Scheme 2). This contrasts the formation of the dicationic cluster $[(\text{Cp}^*\text{Ru})_4(\mu_3\text{-S})_4]\text{Cl}_2$ from **1** under similar conditions.¹⁰ The thermolysis product from the hydrosulfido complexes seems to depend on the ease of oxidation of the neutral clusters $[(\text{Cp}^*\text{M})_4(\mu_3\text{-S})_4]$ ($\text{M} = \text{Ru}, \text{Ir}, \text{Rh}$). Studies on chemical and electrochemical oxidation of these clusters clearly support this idea. The $E_{1/2}$ values for oxidation ($\text{Ru} -0.71$ and -0.28 V; $\text{Ir} -0.46$ and -0.19 V; $\text{Rh} -0.33$ and $+0.29$ V vs SCE) show that the ruthenium cluster **3** is more easily oxidized than the corresponding iridium and rhodium clusters $[(\text{Cp}^*\text{M})_4(\mu_3\text{-S})_4]$ ($\text{M} = \text{Ir}, \text{Rh}$). Actually, the neutral ruthenium cluster **3** immediately reacted with an excess of hydrogen chloride, even at room temperature, giving the dicationic cluster $[(\text{Cp}^*\text{Ru})_4(\mu_3\text{-S})_4]\text{Cl}_2$ in good yield. Thus, the formation of the cationic cluster $[(\text{Cp}^*\text{Ru})_4(\mu_3\text{-S})_4]\text{Cl}_2$ from **1** can be explained by the oxidation of **3** with hydrogen chloride, which is concomitantly generated with **3** from **1**.

(8) (a) Hidai, M.; Mizobe, Y.; Matsuzaka, H. *J. Organomet. Chem.* **1994**, *473*, 1. (b) Hidai, M.; Mizobe, Y. In *Transition Metal Sulfur Chemistry*; Stiefel, E. I., Matsumoto, K., Eds.; American Chemical Society: Washington, DC, 1996; p 310. (c) Takagi, Y.; Matsuzaka, H.; Ishii, Y.; Hidai, M. *Organometallics* **1997**, *16*, 4445. (d) Nishibayashi, Y.; Yamanashi, M.; Takagi, Y.; Hidai, M. *Chem. Commun.* **1997**, 859.

(9) (a) Nishio, M.; Matsuzaka, H.; Mizobe, Y.; Hidai, M. *Angew. Chem., Int. Ed. Engl.* **1996**, *35*, 872. (b) Nishio, M.; Matsuzaka, H.; Mizobe, Y.; Hidai, M. *Inorg. Chim. Acta* **1997**, *263*, 119. (c) Nishio, M.; Mizobe, Y.; Matsuzaka, H.; Hidai, M. *Inorg. Chim. Acta* **1997**, *265*, 59.

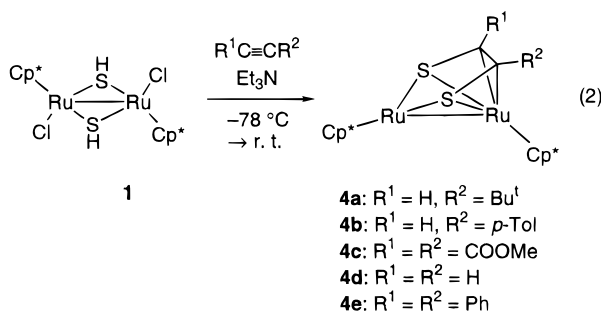
(10) Hashizume, K.; Mizobe, Y.; Hidai, M. *Organometallics* **1996**, *15*, 3303.

(11) (a) Tang, Z.; Nomura, Y.; Ishii, Y.; Mizobe, Y.; Hidai, M. *Organometallics* **1997**, *16*, 151. (b) Tang, Z.; Nomura, Y.; Ishii, Y.; Mizobe, Y.; Hidai, M. *Inorg. Chim. Acta* **1998**, *267*, 73.

(12) Liu, H.; Tan, A. L.; Mok, K. F.; Mak, T. C. W.; Batsanov, A. S.; Howard, J. A. K.; Hor, T. S. A. *J. Am. Chem. Soc.* **1997**, *119*, 11006 and references therein.

(13) Houser, E. J.; Dev, S.; Ogilvy, A. E.; Rauchfuss, T. B.; Wilson, S. R. *Organometallics* **1993**, *12*, 4678.

Trapping of $[\text{Cp}^*\text{Ru}(\mu_2\text{-S})_2\text{RuCp}^*]$ with Alkynes. Formation of Dithiolene-Bridged Diruthenium Complexes. Formation of the cubane-type cluster **3** from **1** described above suggests that the coordinatively unsaturated intermediate $[\text{Cp}^*\text{Ru}(\mu_2\text{-S})_2\text{RuCp}^*]$ is generated upon thermolysis of **1** or treatment of **1** with base. As to a related reaction, Rauchfuss and co-workers have demonstrated that the reactions of $[(\text{Cp}^{\text{Et}}\text{Ru})_2(\mu_2\text{-}\eta^1\text{:}\eta^1\text{-S}_2)(\mu_2\text{-}\eta^2\text{:}\eta^2\text{-S}_2)]$ ($\text{Cp}^{\text{Et}} = \eta^5\text{-C}_5\text{Me}_4\text{Et}$) with 2 equiv of PBU_3 in the presence of CO or diphenylacetylene afford $[\text{Cp}^{\text{Et}}\text{Ru}(\text{CO})(\mu_2\text{-S})_2\text{Ru}(\text{CO})\text{Cp}^{\text{Et}}]^{15}$ or $[(\text{Cp}^{\text{Et}}\text{Ru})_2(\mu_2\text{-}\eta^2\text{:}\eta^4\text{-S}_2\text{C}_2\text{Ph}_2)]$,¹⁶ respectively. Although the formation of intermediary $[\text{Cp}^{\text{Et}}\text{Ru}(\mu_2\text{-S})_2\text{RuCp}^{\text{Et}}]$ was not mentioned, these reactions seem to involve such a sulfido-bridged species and stimulated us to investigate the trapping of $[\text{Cp}^*\text{Ru}(\mu_2\text{-S})_2\text{RuCp}^*]$ generated from the hydrosulfido complex **1** with unsaturated organic molecules. As expected, dehydrohalogenation of **1** in the presence of an excess of alkynes afforded the dithiolene-bridged diruthenium complexes $[(\text{Cp}^*\text{Ru})_2(\mu_2\text{-}\eta^2\text{:}\eta^4\text{-S}_2\text{C}_2\text{-RR}')]$ (**4**; eq 2). Although the isolated yield of **4** was



moderate because of the high solubility of **4** in common organic solvents, the reactions proceeded cleanly for **4a–d** by ^1H NMR. On the other hand, diphenylacetylene was less reactive and a large amount of the cubane-type cluster **3** was isolated along with the dithiolene complex **4e** from the reaction mixture. The ^1H NMR spectra of **4** exhibit two inequivalent singlets due to the Cp^* methyl protons with the same intensity. The signals for the hydrogen atoms attached to the dithiolene ring also appear at 5–6 ppm for **4a**, **4b**, and **4d**. In the $^{13}\text{C}\{^1\text{H}\}$ NMR spectra, the signals ascribed to the ring carbon atoms in the dithiolene ligands are observed in the range of 85–125 ppm, which is considerably higher field than those for other dithiolene complexes (130–180 ppm).¹⁷

Addition of alkynes to metal sulfido complexes has been established as a synthetic method for dithiolene complexes.^{18,19} However, the alkynes employed are usually limited to those activated by electron-withdrawing substituents. Preparation of dithiolene complexes from acetylene or alkynes with electron-donating alkyl substituents are only achieved by using a few highly

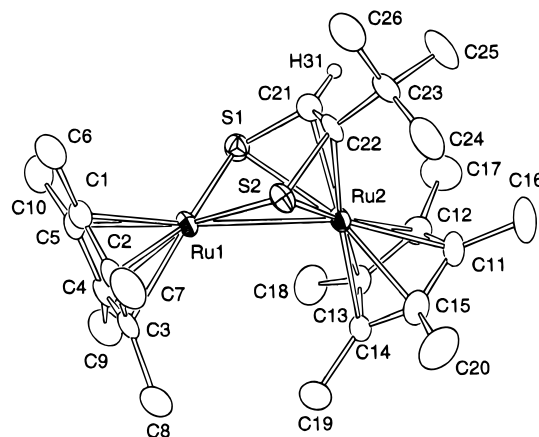


Figure 1. Molecular structure of **4a** with atom-numbering scheme.

Table 1. Selected Interatomic Distances (Å) for **4a** and **5a**

	4a	5a
Ru(1)–Ru(2)	2.993(2)	3.6547(6)
Ru(1)–S(1)	2.271(2)	2.3785(9)
Ru(1)–S(2)	2.262(2)	2.394(1)
Ru(2)–S(1)	2.437(2)	2.407(1)
Ru(2)–S(2)	2.428(2)	2.4273(9)
Ru(2)–C(21)	2.165(6)	2.135(3)
Ru(2)–C(22)	2.204(6)	2.176(3)
S(1)–C(21)	1.738(6)	1.746(4)
S(2)–C(22)	1.772(5)	1.773(3)
C(21)–C(22)	1.399(7)	1.398(4)

reactive complexes.¹⁸ As to alkylacetylenes, only 2-butyne is known to react with ReS_4^- and S_8 to give the bis(dithiolene) complex $[\text{ReS}(\text{S}_2\text{C}_2\text{Me}_2)_2]^-$.²⁰ Interestingly, complex **1** readily reacted with a variety of alkynes including 3,3-dimethyl-1-butyne and acetylene to form dithiolene complexes in the presence of triethylamine under very ambient conditions. This suggests a high reactivity of the sulfido-bridged species $[\text{Cp}^*\text{Ru}(\mu_2\text{-S})_2\text{RuCp}^*]$. On the other hand, the parent **1** itself did not react with these unactivated alkynes at room temperature, although a highly activated alkyne, dimethyl acetylenedicarboxylate, did react with **1** in the absence of triethylamine to give the dithiolene-bridged complex **4c** in low yield. It is to be noted that the preparation of the Cp^{Et} analogue $[(\text{Cp}^{\text{Et}}\text{Ru})_2(\mu_2\text{-}\eta^2\text{:}\eta^4\text{-S}_2\text{C}_2\text{Ph}_2)]$ reported by Rauchfuss et al. requires more forcing conditions (70 °C) compared with that described here.

Trapping of $[\text{Cp}^*\text{Ru}(\mu_2\text{-S})_2\text{RuCp}^*]$ with other unsaturated organic molecules such as alkenes and nitriles was also attempted; however, this resulted in the formation of only the cubane-type cluster **3**. Analogous dehydrohalogenation of the iridium and rhodium complexes **2** with triethylamine in the presence of *p*-tolylacetylene also afforded the cubane-type clusters $[(\text{Cp}^*\text{M})_4(\mu_3\text{-S})_4]$ ($\text{M} = \text{Ir}, \text{Rh}$) exclusively.

An X-ray analysis of $[(\text{Cp}^*\text{Ru})_2(\mu_2\text{-}\eta^2\text{:}\eta^4\text{-S}_2\text{C}_2\text{HBU}^t)]$ (**4a**) has disclosed the dithiolene-bridged dinuclear structure of **4**. The molecular structure is shown in Figure 1, whereas selected bond distances and angles are listed in Table 1. The structure of **4a** closely resembles that of $[(\text{Cp}^{\text{Et}}\text{Ru})_2(\mu_2\text{-}\eta^2\text{:}\eta^4\text{-S}_2\text{C}_2\text{Ph}_2)]$ ¹⁶ and the

(14) Venturelli, A.; Rauchfuss, T. B. *J. Am. Chem. Soc.* **1994**, *116*, 4824.

(15) Ogilvy, A. E.; Rauchfuss, T. B. *Organometallics* **1988**, *7*, 1884.

(16) Rauchfuss, T. B.; Rodgers, D. P. S.; Wilson, S. R. *J. Am. Chem. Soc.* **1986**, *108*, 3114.

(17) Inomata, S.; Takano, H.; Hiyama, K.; Tobita, H.; Ogino, H. *Organometallics* **1995**, *14*, 2112.

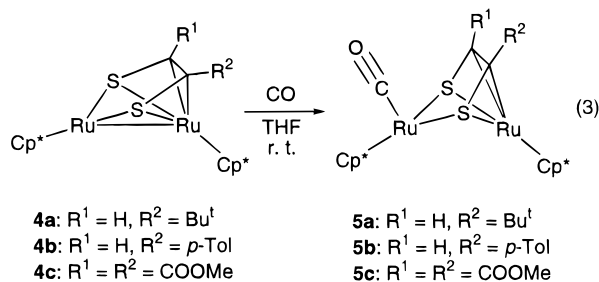
(18) Rakowski DuBois, M.; Jagirdar, B. R.; Dietz, S.; Noll, B. C. *Organometallics* **1997**, *16*, 294 and references therein.

(19) Kawaguchi, H.; Yamada, K.; Lang, J.-P.; Tatsumi, K. *J. Am. Chem. Soc.* **1997**, *119*, 10346.

(20) Goodman, J. T.; Inomata, S.; Rauchfuss, T. B. *J. Am. Chem. Soc.* **1996**, *118*, 11674.

isoelectronic dimanganese complex $[\{\text{Mn}(\text{CO})_3\}_2(\mu_2\text{-}\eta^2\text{:}\eta^4\text{-S}_2\text{C}_2\text{Ph}_2)]$.²¹ The dithiolene ligand bridges the two ruthenium atoms unsymmetrically: it binds to the Ru(1) atom through only two sulfur atoms whereas it binds to the Ru(2) atom through all four atoms in the dithiolene ligand. The distances of Ru(1)–S (2.262(2) and 2.271(2) Å) are shorter than those of Ru(2)–S (2.428(2) and 2.437(2) Å). A similar unsymmetrical bridging has been deduced for the related diruthenium benzenedithiolato complex $[\text{Cp}^*\text{Ru}(\mu_2\text{-S}_2\text{C}_6\text{H}_4)\text{RuCp}^*]$ from its ¹H NMR spectrum.²² The Ru–Ru distance of 2.993(2) Å is significantly longer than those observed in thiolato-bridged diruthenium complexes with a Ru–Ru single bond (2.6–2.9 Å)⁸ but still indicates a Ru–Ru interaction. This is congruent with the effective atomic number (EAN) rule if the bridging dithiolene ligand is regarded as a neutral eight-electron donor. The dithiolene ring in **4a** is almost completely planar, as in the isoelectronic complexes mentioned above: the dihedral angle between the plane of S(1)–Ru(1)–S(2) and the least-squares plane of S(1)–C(21)–C(22)–S(2) is 7.9°.

Preparation and Structure of $[\text{Cp}^*\text{Ru}(\text{CO})(\mu_2\text{-}\eta^2\text{:}\eta^4\text{-S}_2\text{C}_2\text{RR}')\text{RuCp}^*]$ (5**).** When solutions of the dithiolene-bridged diruthenium complexes **4** were stirred under a CO atmosphere, the carbonyl complexes $[\text{Cp}^*\text{Ru}(\text{CO})(\mu_2\text{-}\eta^2\text{:}\eta^4\text{-S}_2\text{C}_2\text{RR}')\text{RuCp}^*]$ (**5**) were obtained in good yield (eq 3). A strong band ascribed to the terminally



bound carbonyl ligand is observed around 1900 cm⁻¹ in the IR spectra of **5**. The ¹H and ¹³C{¹H} spectra clearly demonstrate the presence of the dithiolene ligand: the resonances for the hydrogen atoms attached to the dithiolene ring appear at 5–7 ppm and those for the ring carbon atoms in the dithiolene ligands in the range of 80–125 ppm. It is worth mentioning that the iron analogue of **5**, $[\text{Cp}^*\text{Fe}(\text{CO})\{\mu_2\text{-}\eta^2\text{:}\eta^4\text{-S}_2\text{C}_2(\text{COOMe})_2\}\text{FeCp}^*]$, has been isolated in low yield from the reaction of $[\text{Cp}^*\text{Fe}_2(\text{CO})_4]$ with elemental sulfur and dimethyl acetylenedicarboxylate.¹⁷

An X-ray analysis of $[\text{Cp}^*\text{Ru}(\text{CO})(\mu_2\text{-}\eta^2\text{:}\eta^4\text{-S}_2\text{C}_2\text{HBu}^t)\text{RuCp}^*]$ (**5a**) has been undertaken to compare the structures of both **4** and **5** in detail (Figure 2). In contrast to **4a**, the Ru(1)–Ru(2) distance of 3.6547(6) Å precludes any metal–metal bonding. Coordination of CO also affected the bridging manner of the dithiolene ligand. Although the ligand still bridges the two ruthenium atoms in an $\eta^2\text{:}\eta^4$ -coordination mode, the dithiolene ring in **5a** is now folded with a dihedral angle of 40.9° along the S(1)–S(2) vector and the distances of

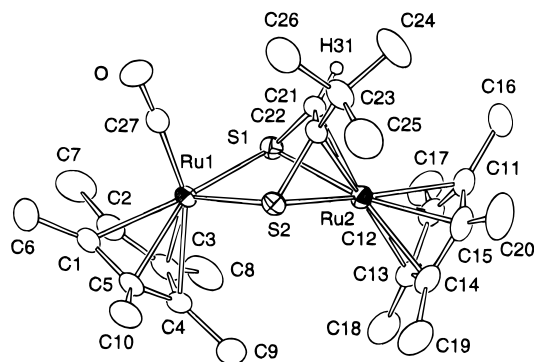
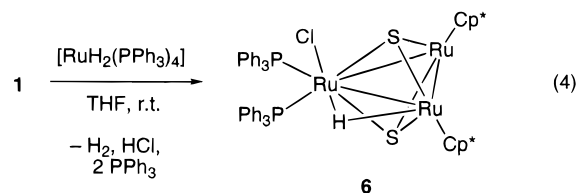


Figure 2. Molecular structure of **5a** with atom-numbering scheme.

Ru(1)–S and Ru(2)–S become essentially equal. These features are common with $[\text{Cp}^*\text{Fe}(\text{CO})\{\mu_2\text{-}\eta^2\text{:}\eta^4\text{-S}_2\text{C}_2(\text{COOMe})_2\}\text{FeCp}^*]$, whose dithiolene and CO ligands are, however, mutually *trans*-orientated. The dihedral angle between the two Ru₂S planes in **5a** (143.44°) is significantly larger than that in **4a** (116.03°). It is of interest that the dithiolato complex $[\text{Cp}^*\text{Ru}(\mu_2\text{-}\eta^2\text{:}\eta^4\text{-S}_2\text{C}_6\text{H}_4)]$ is also known to react with CO or P(OMe)₃ to give the closely related diruthenium complexes $[\text{Cp}^*\text{RuL}(\mu_2\text{-}\eta^2\text{:}\eta^4\text{-S}_2\text{C}_6\text{H}_4)\text{RuCp}^*]$ (L = CO, P(OMe)₃), the latter of which has a similar cis orientation of the dithiolato and phosphite ligands that has been confirmed by X-ray crystallography.²²

Preparation and Structure of $[(\text{Cp}^*\text{Ru})_2(\mu_3\text{-S})_2(\mu_2\text{-H})\text{RuCl}(\text{PPh}_3)_2]$ (6**).** We have previously found that the hydrosulfido-bridged diruthenium complex **1** reacts with $[\text{RhCl}(\text{PPh}_3)_3]$ to give the heterometallic sulfido cluster $[(\mu_2\text{-H})(\text{Cp}^*\text{Ru})_2(\mu_3\text{-S})_2\text{RhCl}_2(\text{PPh}_3)]$.¹⁰ Similarly, the reaction of **1** with a nearly equimolar amount of $[\text{RuH}_2(\text{PPh}_3)_4]$ resulted in the formation of the sulfido-capped triruthenium cluster $[(\text{Cp}^*\text{Ru})_2(\mu_3\text{-S})_2(\mu_2\text{-H})\text{RuCl}(\text{PPh}_3)_2]$ (**6**) in moderate yield (eq 4). Concomitant

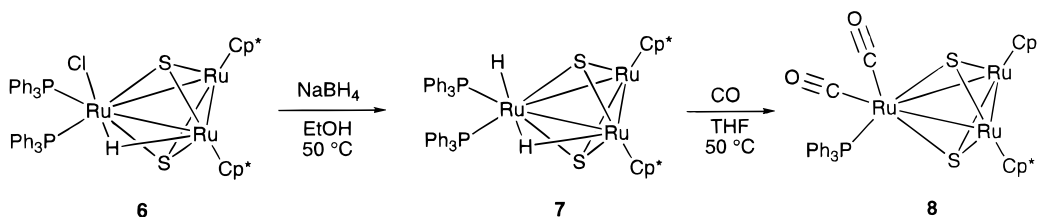


evolution of H₂ has been confirmed by GLC analysis. The ¹H NMR spectrum of **6** exhibits a high-field hydrido resonance split by two equivalent phosphorus nuclei as well as two inequivalent singlets ascribed to the Cp* methyl protons. The ³¹P{¹H} NMR spectrum also demonstrates the equivalence of the two phosphine ligands. On the other hand, no band ascribed to ν_{RuH} is observed in the IR spectrum. These spectroscopic data suggest that the hydrido ligand bridges the two ruthenium atoms, one originating from **1** and the other from incorporated ruthenium atom. In contrast, the hydrido ligand in $[(\mu_2\text{-H})(\text{Cp}^*\text{Ru})_2(\mu_3\text{-S})_2\text{RhCl}_2(\text{PPh}_3)]$ bridges two ruthenium atoms and shows no coupling with rhodium and phosphorus nuclei in the ¹H NMR spectrum.¹⁰ It is also worth mentioning that when $[\text{RuH}_2(\text{PPh}_3)_4]$ is treated with the hydrosulfido-bridged diiridium complex **2a** in place of **1**, the triangular cluster $[(\text{Cp}^*\text{Ir})_2(\mu_3\text{-S})_2\text{RuCl}_2(\text{PPh}_3)]$ with no hydrido ligand is obtained.²³

(21) Lindner, E.; Butz, I. P.; Hoehne, S.; Hiller, W.; Fawzi, R. *J. Organomet. Chem.* **1983**, 259, 99.

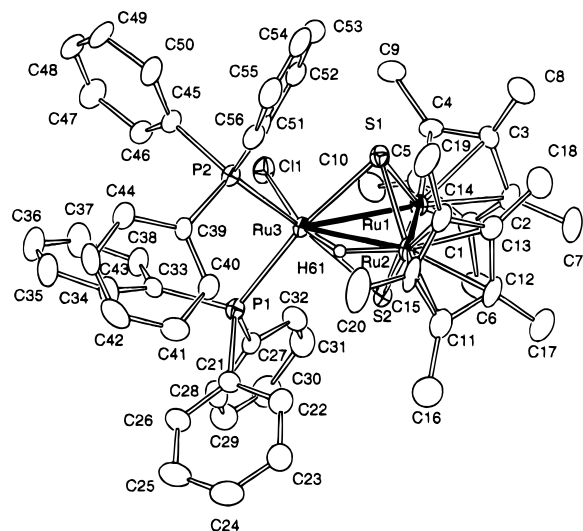
(22) Hörnig, A.; Englert, U.; Kölle, U. *J. Organomet. Chem.* **1994**, 464, C25.

Scheme 3

**Table 2.** Selected Bond Distances (Å) and Angles (deg) for 6–8

	6·0.5THF	7·THF	8
Distances			
Ru(1)–Ru(2)	2.842(1)	2.811(3)	2.858(1)
Ru(1)–Ru(3)	2.868(1)	2.818(2)	2.841(1)
Ru(2)–Ru(3)	2.778(1)	2.814(2)	2.827(2)
Ru(1)–S(1)	2.233(3)	2.241(1)	2.243(3)
Ru(1)–S(2)	2.235(3)	2.233(1)	2.271(3)
Ru(2)–S(1)	2.287(3)	2.291(1)	2.274(3)
Ru(2)–S(2)	2.300(3)	2.309(1)	2.275(3)
Ru(3)–S(1)	2.372(3)	2.360(1)	2.378(3)
Ru(3)–S(2)	2.376(2)	2.390(1)	2.400(3)
Ru(3)–P(1)	2.391(3)	2.325(1)	2.313(4)
Ru(3)–P(2)	2.424(3)	2.303(1)	
Ru(3)–H _b ^a	1.67	1.67(4)	
Ru(2)–H _b ^a	1.48	1.74(4)	
Ru(3)–H(69)		1.52(4)	
Angles			
Ru(2)–Ru(1)–Ru(3)	58.21(3)	58.91(2)	59.46(3)
Ru(1)–Ru(2)–Ru(3)	61.35(3)	59.66(1)	59.97(3)
Ru(1)–Ru(3)–Ru(2)	60.44(3)	61.43(2)	60.56(4)

^a H_b = H(61) (6·0.5THF) or H(70) (7·THF).

**Figure 3.** Molecular structure of 6·0.5THF with atom-numbering scheme. Solvating THF is omitted for clarity.

The trinuclear structure of **6** has unequivocally been established by X-ray crystallography; an ORTEP drawing is shown in Figure 3, and selected bond distances and angles are listed in Table 2. Cluster **6** has a triangular Ru₃ core capped by two μ_3 -S ligands from both sides. The hydrido ligand, which has been found in the final difference Fourier map, bridges the Ru(2) and Ru(3) atoms. Neglecting the Ru–Ru interactions, the coordination geometry around the Ru(3) atom is distorted octahedral with the H and Cl ligands in mutually trans positions. As expected from the EAN

rule, there are three Ru–Ru single bonds in **6**, whose distances at 2.778(1)–2.868(1) Å are comparable to those in an isoelectronic Ru(II)/Ru(III)/Ru(III) cluster [(Cp*₃Ru)₃(μ_3 -S)₂(μ_2 -H)] (2.798(2)–2.851(3) Å)²⁴ and slightly shorter than those in Ru(II)/Ru(II)/Ru(II) clusters [(Cp*₃Ru)₃(μ_3 -S)(μ_3 -X)] (X = Cl, SPrⁱ; 2.874(2)–2.9599(9) Å).²⁴ The two μ_3 -S ligands are located closer to the Ru(1) and Ru(2) atoms than to the Ru(3) atom: the distances from these S atoms to the former ruthenium atoms (2.233(3)–2.300(3) Å) are slightly shorter than those to the latter (2.372(3) and 2.376(2) Å).

Thus, the present study has again shown that the hydrosulfido-bridged dinuclear complex **1** as well as its iridium and rhodium analogues **2** can serve as a good precursor to the clusters with higher nuclearity. It should be emphasized that the triruthenium cluster **6** prepared through this synthetic pathway has different types of terminal ligands, in contrast to the clusters with Ru₃(μ_3 -S)₂ cores reported so far, including [(Cp*₃Ru)₃(μ_3 -S)₂(μ_2 -H)]²⁴ and [(*p*-cymene)₃Ru₃(μ_3 -S)₂]ⁿ⁺ (*n* = 0, 2).²⁵

Preparation and Structure of [(Cp*₂Ru)₂(μ_3 -S)₂(μ_2 -H)RuH(PPh₃)₂] (7). Cluster **6** has labile Cl and PPh₃ ligands along with tightly bound Cp* ligands. Thus site-specific substitution is expected to occur in **6**. Indeed, when the mixture of **6** and an excess of NaBH₄ in ethanol was heated at 50 °C, the dihydrido cluster [(Cp*₂Ru)₂(μ_3 -S)₂(μ_2 -H)RuH(PPh₃)₂] (**7**) was obtained in high yield (Scheme 3). Contrary to the solid-state structure (vide infra), the ¹H NMR spectrum of **7** exhibits one sharp singlet due to the Cp* methyl protons, even at –50 °C, indicating the fluxional behavior of the terminal and bridging hydrido ligands in solution. The spectrum also shows only one high-field hydrido resonance with the intensity of 2 H, which is split into a triplet by two equivalent phosphorus nuclei; the equivalence of two phosphine ligands is further supported by the ³¹P{¹H} NMR spectrum. The IR spectrum shows a characteristic band at 1919 cm^{–1}, which is assignable to stretching of the Ru–H bond.

An X-ray analysis has been carried out to clarify the detailed structure of **7**; an ORTEP drawing of **7** is depicted in Figure 4, and selected bond distances and angles are listed in Table 2. Cluster **7** has essentially the same (Cp*₂Ru)₂(μ_3 -S)₂Ru core as **6**. The two hydrido ligands have been found in the final Fourier map; one of them (H(69)) is bound to Ru(3) as a terminal ligand, whereas the other (H(70)) bridges the Ru(2) and Ru(3) atoms. Replacement of the chloro ligand in **6** with a sterically less demanding hydrido ligand has changed the coordination geometry around the Ru(3) atom slightly: the P(2) atom, which is on the opposite side of

(24) Hashizume, K.; Mizobe, Y.; Hidai, M. *Organometallics* **1995**, *14*, 5367.

(25) Lockemeyer, J. R.; Rauchfuss, T. B.; Rheingold, A. L. *J. Am. Chem. Soc.* **1989**, *111*, 5733.

(23) Tang, Z.; Ishii, Y.; Mizobe, Y.; Hidai, M. Unpublished results.

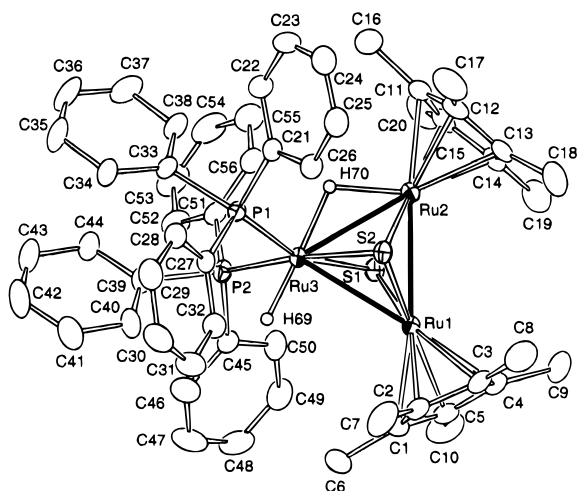


Figure 4. Molecular structure of **7**·THF with atom-numbering scheme. Solvating THF is omitted for clarity.

the chloro ligand as to the Ru(3)–S(1)–S(2) plane in **6** (1.04 Å apart from the plane), has come to the same side of the terminal hydrido ligand (0.17 Å apart from the plane).

Preparation and Structure of [(Cp*Ru)₂(μ₃-S)₂Ru(CO)₂(PPh₃)₃] (8**).** Reaction of **7** with CO (1 atm) at 50 °C resulted in the formation of the Ru(II)/Ru(II)/Ru(II) dicarbonyl cluster [(Cp*Ru)₂(μ₃-S)₂Ru(CO)₂(PPh₃)₃] (**8**) in 35% yield (Scheme 3). The ¹H NMR spectrum of **8** shows the presence of Cp* and PPh₃ ligands in a ratio of 2:1 and the absence of hydrido ligands. Two strong bands at 1970 and 1921 cm⁻¹ ascribed to ν_{CO} are observed in the IR spectrum; the wavenumbers are slightly lower than those of the Ru(II) complex *cct*-[RuCl₂(CO)₂(PPh₃)₂] (2050 and 1990 cm⁻¹),²⁶ suggesting that the (Cp*Ru)₂(μ₃-S)₂Ru fragment in **8** is more electron donating than the RuCl₂(PPh₃) one. It may be noted that the reaction of [RuH₂(PPh₃)₄]^{27a} or [RuH₂(N₂)(PPh₃)₃]^{27b} with CO gives only [RuH₂(CO)(PPh₃)₃], and replacement of H₂ with CO does not occur, at least, at room temperature. The isoelectronic clusters [(Cp*Fe)₂(μ₃-S)₂M(CO)₃] (M = Fe, Ru) have been prepared from the reaction of [(Cp*Fe)₂(μ₂-η¹:η¹-S₂)(μ₂-η²:η²-S₂)] with the corresponding metal carbonyl complexes.²⁸

The molecular structure of **8** determined by X-ray analysis is depicted in Figure 5, and selected bond distances and angles are listed in Table 2, which clearly shows that the (Cp*Ru)₂(μ₃-S)₂Ru core in **6** and **7** has been retained in **8**. However, the coordination geometry around the Ru(3) atom is now trigonal bipyramidal with the S(2) and P atoms at the two apical positions. The three Ru(II)–Ru(II) single bond distances at 2.827(2)–2.858(1) Å are still comparable to the Ru–Ru distances in Ru(III)/Ru(III)/Ru(II) clusters **6**, **7**, and [(Cp*Ru)₃(μ₃-S)₂(μ₂-H)] (2.778(1)–2.868(1) Å) rather than those in Ru(II)/Ru(II)/Ru(II) clusters (vide supra).

Conclusion

We have demonstrated that the hydrosulfido-bridged diruthenium complex **1** serves as a useful precursor to

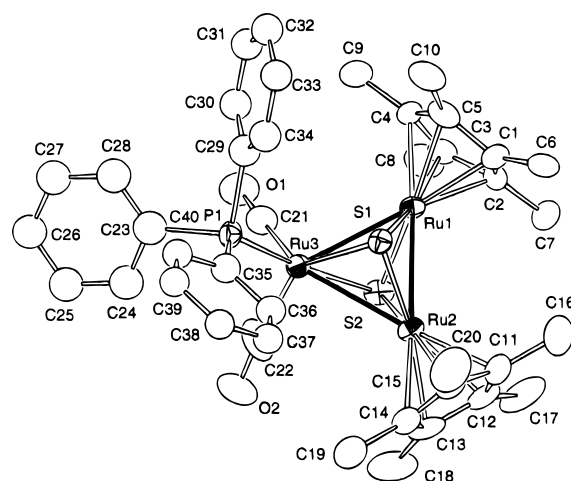


Figure 5. Molecular structure of **8** with atom-numbering scheme. Only one of the disordered components is shown for the phenyl rings.

not only the dithiolene-bridged diruthenium complexes **4** but also the tri- and tetraruthenium sulfido clusters **6** and **3**, all of which contain the Cp*Ru(μ-S)₂RuCp* fragment. These reactivities of **1** strongly suggest the formation of the coordinatively unsaturated sulfido-bridged intermediate [Cp*Ru(μ₂-S)₂RuCp*] upon treatment of **1** with base. Formation of such an intermediate is common with the corresponding diiridium and dirhodium complexes **2**. It may be considered that α-dehydrohalogenation of hydrosulfido-bridged dinuclear complexes with base provides a general method to afford coordinatively unsaturated sulfido-bridged dinuclear centers. These intermediary species readily dimerize in the absence of substrates to give the cubane-type clusters [(Cp*M)₄(μ₃-S)₄] (M = Ru, Ir, Rh). In the presence of alkynes, the intermediary species [Cp*Ru(μ₂-S)₂RuCp*] is transformed into the dithiolene-bridged diruthenium complexes **4**, which further reacts with CO to give the carbonyl complexes **5**. The triruthenium sulfido cluster **6** with a chloride anion and a bridging hydrido ligand undergoes site-specific ligand substitution to give the dihydrido cluster **7**, which has further been converted to the dicarbonyl cluster **8** under CO; the (Cp*Ru)₂(μ₃-S)₂Ru core is retained throughout these reactions.

Experimental Section

General Comments. All manipulations were performed under an atmosphere of nitrogen or argon using standard Schlenk techniques. Solvents were dried by refluxing over Na/benzophenone ketyl (THF, toluene, benzene, and diethyl ether), Mg(OEt)₂ (ethanol), or Mg(OMe)₂ (methanol) and distilled before use. Triethylamine was distilled from sodium, whereas alkynes were used as received. IR spectra were recorded on a Shimadzu 8100M spectrometer. ¹H (270 MHz), ¹³C{¹H} (67.8 MHz), and ³¹P{¹H} (109 MHz) NMR spectra were recorded in C₆D₆ on a JEOL EX-270 spectrometer; chemical shifts are referenced to the signals of the residual nondeuterated benzene at 7.2 ppm (¹H), C₆D₆ at 128.7 ppm (¹³C), and PPh₃ in CDCl₃ at -5.65 ppm (85% H₃PO₄ = 0.0 ppm; ³¹P). Hydrogen gas evolution was determined by GLC analysis using a Shimadzu GC-8A gas chromatograph equipped with a molecular sieve 13X column. Electrochemical measurements were made with Hokuto Denko instrumentation (HA-501 potentiostat and HB-105 function generator) using a glassy

(26) Collman, J. P.; Roper, W. R. *J. Am. Chem. Soc.* **1965**, *87*, 4008.

(27) (a) Harris, R. O.; Hota, N. K.; Sadaroy, L.; Yuen, J. M. C. *J. Organomet. Chem.* **1973**, *54*, 259. (b) Knoth, W. H. *J. Am. Chem. Soc.* **1972**, *94*, 104.

(28) Mitsui, T.; Inomata, S.; Ogino, H. *Inorg. Chem.* **1994**, *33*, 4934.

carbon working electrode; potentials were measured in CH₂-Cl₂-0.1 M Buⁿ₄NBF₄ vs a saturated calomel electrode as the reference. Elemental analyses were performed on a Perkin-Elmer 2400II CHN analyzer or at the Elemental Analysis Laboratory, Department of Chemistry, The University of Tokyo.

Preparation of [(CpRu*)₂(μ₃-S)₄] (3).** To a toluene solution (12 mL) of **1** (82.7 mg, 0.136 mmol) was added triethylamine (0.11 mL, 0.79 mmol) at -78 °C, and the mixture was slowly warmed to room temperature with stirring. The solvent was then removed in vacuo, and the resultant dark brown solid was recrystallized from THF-methanol (2 mL/2 mL) at -23 °C, affording **3** as a brown solid (32.3 mg, 44%). ¹H NMR: δ 1.77 (s, 60 H, C₅Me₅; literature value δ 1.72¹³). Anal. Calcd for C₄₀H₆₀Ru₄S₄: C, 44.76; H, 5.63; S, 11.95; Cl, 0. Found: C, 44.62; H, 5.79; S, 11.14; Cl, 0.

Reaction of 3 with HCl. To a solution of **3** (51.4 mg, 0.0478 mmol) in toluene (10 mL) was bubbled HCl gas for 10 s, and the mixture was stirred for 1 h at room temperature. The dark brown solid precipitated was filtered off, washed with diethyl ether, and dried in vacuo to give 47.9 mg of [(Cp**Ru*)₄(μ₃-S)₄]Cl₂ (82%).¹⁰

Thermolysis of [CpIr*Cl(μ₂-SH)₂IrClCp*] (2a).** A toluene (10 mL) solution of **2a** (84.1 mg, 0.106 mmol) was heated at reflux for 7 h. The resultant orange suspension was dried, then extracted with benzene (30 mL). Removal of the solvent from the extract afforded 39.4 mg of [(Cp**Ir*)₄(μ₃-S)₄]^{2f,29} as an orange powder (52%). Similar treatment of **2b** gave [(Cp**Rh*)₄(μ₃-S)₄]³⁰ in 42% yield.

Preparation of [(CpRu*)₂(μ₂-η²:η⁴-S₂C₂RR')RuCp*] (4).** The following procedure for the preparation of [(Cp**Ru*)₂(μ₂-η²:η⁴-S₂C₂HBU^t)] (**4a**) is representative. To a solution of **1** (409.1 mg, 0.671 mmol) in THF (18 mL) was added triethylamine (0.55 mL, 4.0 mmol) and Bu^tCCH (0.50 mL, 4.1 mmol) at -78 °C, and the mixture was slowly warmed to room temperature with stirring. The resultant red solution was evaporated in vacuo, and the residue was extracted with benzene (20 mL). Addition of methanol to the concentrated extract gave **4a** as red crystals (183.7 mg, 44%). ¹H NMR: δ 5.42 (s, 1 H, S₂C₂HBU^t), 2.05, 1.84 (s, 15 H each, C₅Me₅), 1.36 (s, 9 H, CMe₃). ¹³C{¹H} NMR: δ 122.9, 86.5 (S₂C₂HBU^t), 88.6, 83.4 (C₅Me₅), 37.4 (CMe₃), 33.4 (CMe₃), 13.3, 13.2 (C₅Me₅). Anal. Calcd for C₂₆H₄₀S₂Ru₂: C, 50.46; H, 6.51. Found: C, 50.03; H, 6.68.

[(CpRu*)₂(μ₂-η²:η⁴-S₂C₂HTol)] (4b).** Yield: 75%. ¹H NMR: δ 7.69, 6.94 (d, 2 H each, *J* = 8.1 Hz, C₆H₄), 5.74 (s, 1 H, S₂C₂HTol), 2.11 (s, 3 H, C₆H₄Me), 2.08, 1.62 (s, 15 H each, C₅Me₅). ¹³C{¹H} NMR: δ 138.0, 136.6 (*ipso*-C), 129.6, 127.9 (*o*- and *m*-C), 104.0, 85.6 (S₂C₂HTol), 88.8, 83.9 (C₅Me₅), 21.8 (C₆H₄Me), 13.3, 11.9 (C₅Me₅). Anal. Calcd for C₂₉H₃₈S₂Ru₂: C, 53.35; H, 5.87. Found: C, 53.07; H, 5.86.

[(CpRu*)₂(μ₂-η²:η⁴-S₂C₂(COOMe)₂)] (4c).** Yield: 39%. IR (KBr): 1698, 1730 cm⁻¹ (s, ν_{C=O}). ¹H NMR: δ 3.52 (s, 6 H, COOMe), 1.90, 1.83 (s, 15 H each, C₅Me₅). ¹³C{¹H} NMR: δ 171.4 (COOMe), 97.7 (S₂C₂(COOMe)₂), 92.6, 85.5 (C₅Me₅), 52.7 (COOMe), 13.0, 11.5 (C₅Me₅). Anal. Calcd for C₂₆H₃₆O₄S₂Ru₂: C, 46.00; H, 5.35. Found: C, 45.77; H, 5.52. Complex **4c** was also obtained from the reaction of **1** (79.3 mg, 0.130 mmol) and dimethyl acetylenedicarboxylate (60 μL, 0.49 mmol) in THF (10 mL) at room temperature for 21 h. Recrystallization from benzene-methanol (1 mL/2 mL) afforded **4c** in 19% yield.

[(CpRu*)₂(μ₂-η²:η⁴-S₂C₂H₂)] (4d).** Acetylene gas was bubbled for 10 min into a mixture of **1** and triethylamine in THF at -78 °C. The mixture was treated as described above, and recrystallization from methanol at -23 °C afforded **4d** in 60% yield. ¹H NMR: δ 5.12 (s, 2 H, S₂C₂H₂), 2.06, 1.73 (s, 15

H each, C₅Me₅). ¹³C{¹H} NMR: δ 88.44 (S₂C₂H₂), 88.37, 83.7 (C₅Me₅), 13.4, 12.3 (C₅Me₅). Anal. Calcd for C₂₂H₃₂S₂Ru₂: C, 46.95; H, 5.73. Found: C, 46.57; H, 5.99.

[(CpRu*)₂(μ₂-η²:η⁴-S₂C₂Ph₂)] (4e).** The crude reaction mixture obtained as described above was extracted with benzene-hexanes (1:1) and chromatographed on alumina with benzene-hexanes (1:4). Removal of the solvent from the first red band and recrystallization from benzene-methanol afforded red crystals of **4e**, which were washed with a small amount of hexanes and dried in vacuo (7%). ¹H NMR: δ 7.52-6.99 (m, 10 H, Ph), 2.05, 1.70 (s, 15 H each, C₅Me₅). Anal. Calcd for C₂₂H₃₂S₂Ru₂: C, 57.12; H, 5.64. Found: C, 56.91; H, 5.67. Evaporation of the solvent from the second dark red band obtained by using methanol as an eluent afforded **3** in 58% yield.

Preparation of [CpRu*(CO)(μ₂-η²:η⁴-S₂C₂RR')RuCp*] (5).** The following procedure for the preparation of [Cp**Ru*(CO)(μ₂-η²:η⁴-S₂C₂HBU^t)RuCp*] (**5a**) is representative. Through a solution of **4a** (139.6 mg, 0.226 mmol) in THF (10 mL) was bubbled CO for 5 min, and the mixture was stirred for 15 h at room temperature. After removal of the solvent in vacuo, the resultant red solid was recrystallized from benzene-methanol (0.5 mL/3 mL). The red crystals formed were filtered off, washed with a small amount of methanol, and dried in vacuo (112.9 mg, 77%). IR (KBr): 1918 cm⁻¹ (s, ν_{CO}). ¹H NMR: δ 6.17 (s, 1 H, S₂C₂HBU^t), 1.76, 1.67 (s, 15 H each, C₅Me₅), 1.60 (s, 9 H, CMe₃). ¹³C{¹H} NMR: δ 205.2 (CO), 121.9, 84.4 (S₂C₂HBU^t), 94.2, 88.6 (C₅Me₅), 38.1 (CMe₃), 32.1 (CMe₃), 12.7, 10.8 (C₅Me₅). Anal. Calcd for C₂₇H₄₀OS₂Ru₂: C, 50.13; H, 6.23. Found: C, 49.98; H, 6.24.

[CpRu*(CO)(μ₂-η²:η⁴-S₂C₂HTol)RuCp*] (5b).** Yield: 68%. IR (KBr): 1910 cm⁻¹ (s, ν_{CO}). ¹H NMR: δ 7.76, 6.98 (d, 2 H each, *J* = 8.3 Hz, C₆H₄), 6.58 (s, 1 H, S₂C₂HTol), 2.12 (s, 3 H, C₆H₄Me), 1.67, 1.52 (s, 15 H each, C₅Me₅). ¹³C{¹H} NMR: δ 204.8 (CO), 139.6, 136.2 (*ipso*-C), 129.8, 126.5 (*o*- and *m*-C), 102.6, 83.8 (S₂C₂HTol), 94.3, 88.7 (C₅Me₅), 21.9 (C₆H₄Me), 11.4, 10.8 (C₅Me₅). Anal. Calcd for C₃₀H₃₈OS₂Ru₂: C, 52.92; H, 5.63. Found: C, 52.81; H, 5.77.

[CpRu*(CO)(μ₂-η²:η⁴-S₂C₂(COOMe)₂)RuCp*] (5c).** Yield: 89%. IR (KBr): 1929 (s, ν_{CO}), 1721, 1696 cm⁻¹ (s, ν_{C=O}). ¹H NMR: δ 3.58 (s, 6 H, COOMe), 1.75, 1.51 (s, 15 H each, C₅Me₅). ¹³C{¹H} NMR: δ 204.3 (CO), 172.2 (COOMe), 95.3 (S₂C₂(COOMe)₂), 94.2, 93.4 (C₅Me₅), 52.7 (COOMe), 11.1, 10.5 (C₅Me₅). Anal. Calcd for C₂₇H₃₆O₅S₂Ru₂: C, 45.88; H, 5.13. Found: C, 46.27; H, 5.24.

Preparation of [(CpRu*)₂(μ₃-S)₂(μ₂-H)RuCl(PPh₃)₂]-0.5THF (6·0.5THF).** To a solution of **1** (45.7 mg, 0.0750 mmol) in THF (10 mL) was added [RuH₂(PPh₃)₄] (87.8 mg, 0.0762 mmol), and the mixture was stirred for 18 h at room temperature. Evolution of an equimolar amount of H₂ was confirmed by GLC analysis. The resultant brown solution was reduced to 3 mL, and methanol (10 mL) was layered on the solution. The dark brown crystals that formed were filtered off, washed with diethyl ether, and dried in vacuo (51.0 mg, 55%). ¹H NMR: δ 7.68-6.99 (m, 30 H, Ph), 2.09, 1.48 (s, 15 H each, C₅Me₅), -27.97 (t, 1 H, ²J_{PH} = 14.1 Hz, RuH). ³¹P{¹H} NMR: δ 29.5 (s). Anal. Calcd for C₅₈H₆₅O_{0.5}P₂S₂ClRu₃: C, 56.41; H, 5.31. Found: C, 56.58; H, 5.57.

Preparation of [(CpRu*)₂(μ₃-S)₂(μ₂-H)RuH(PPh₃)₂]-THF (7·THF).** To a suspension of **6·0.5THF** (33.9 mg, 0.0283 mmol) in ethanol (8 mL) was added NaBH₄ (22.1 mg, 0.584 mmol), and the mixture was stirred for 8 h at 50 °C. After removal of the solvent in vacuo, the resultant brown solid was extracted with benzene (8 mL). The extract was evaporated to dryness and recrystallized from THF-methanol (1 mL/3 mL). The dark brown crystals that formed were filtered off, washed with methanol, and dried in vacuo (30.3 mg, 89%). IR (KBr): 1919 cm⁻¹ (w, ν_{RuH}). ¹H NMR: δ 7.70-6.97 (m, 30 H, Ph), 1.89 (s, 30 H, C₅Me₅), -16.32 (t, 2 H, ²J_{PH} = 22.6 Hz, RuH). ³¹P{¹H} NMR: δ 61.9 (s). Anal. Calcd for C₆₀H₇₀OP₂S₂Ru₃: C, 58.28; H, 5.71. Found: C, 58.33; H, 5.87.

(29) Herberhold, M.; Jin, G.-X.; Milius, W. *Chem. Ber.* **1995**, *128*, 557.

(30) Skaugset, A. E.; Rauchfuss, T. B.; Wilson, S. R. *Organometallics* **1990**, *9*, 2875.

Table 3. X-ray Crystallographic Data for **4a**, **5a**, **6·0.5THF**, **7·THF**, and **8**

	4a	5a	6·0.5THF	7·THF	8
formula	C ₂₆ H ₄₀ S ₂ Ru ₂	C ₂₇ H ₄₀ OS ₂ Ru ₂	C ₅₈ H ₆₅ P ₂ S ₂ ClRu ₃ O _{0.5}	C ₆₀ H ₇₀ P ₂ S ₂ Ru ₃ O	C ₄₀ H ₄₅ Ru ₃ O ₂ S ₂ P
fw	618.86	646.87	1234.88	1236.49	956.10
cryst syst	monoclinic	triclinic	orthorhombic	triclinic	monoclinic
space group	<i>P</i> 2 ₁ / <i>n</i> (No. 14)	<i>P</i> $\bar{1}$ (No. 2)	<i>Pbca</i> (No. 61)	<i>P</i> $\bar{1}$ (No. 2)	<i>P</i> 2 ₁ / <i>n</i> (No. 14)
cryst color	dark red	dark red	dark brown	dark brown	dark brown
cryst dimens, mm	0.3 × 0.5 × 0.7	0.1 × 0.3 × 0.6	0.1 × 0.2 × 0.6	0.2 × 0.3 × 0.4	0.1 × 0.2 × 0.5
<i>a</i> , Å	11.683(6)	10.745(2)	12.749(8)	12.346(2)	9.738(4)
<i>b</i> , Å	16.509(5)	14.461(2)	22.486(9)	21.675(4)	30.742(4)
<i>c</i> , Å	14.401(3)	10.729(2)	36.846(7)	11.018(2)	13.406(4)
α , deg	90	104.59(1)	90	94.58(2)	90
β , deg	106.22(3)	113.87(1)	90	101.39(2)	97.61(3)
γ , deg	90	69.19(1)	90	73.71(2)	90
<i>V</i> , Å ³	2667(1)	1413.7(4)	10562(6)	2773.5(9)	3977(2)
<i>Z</i>	4	2	8	2	4
<i>D_c</i> , g cm ⁻³	1.541	1.520	1.553	1.481	1.596
<i>F</i> (000), e	1264	660	5024	1264	1920
μ (Mo K α), cm ⁻¹	13.00	12.33	10.76	9.79	13.02
reflms measd	+ <i>h</i> , + <i>k</i> , \pm <i>l</i>	+ <i>h</i> , \pm <i>k</i> , \pm <i>l</i>	+ <i>h</i> , + <i>k</i> , + <i>l</i>	+ <i>h</i> , \pm <i>k</i> , \pm <i>l</i>	+ <i>h</i> , + <i>k</i> , \pm <i>l</i>
no. of unique reflms	3637	4964	7625	8795	7159
transmission factors	0.9127–0.9987	0.6860–1.0000	0.8207–1.0000	0.8389–1.0000	0.5395–1.0000
no. of data used (<i>I</i> > 3 σ (<i>I</i>))	2956	4128	4161	6731	4048
no. variables	272	290	665	620	314
<i>R^a</i>	0.036	0.026	0.043	0.032	0.058
<i>R_w^a</i>	0.027	0.021	0.038	0.025	0.051
GOF ^b	3.62	2.17	1.52	2.00	2.39
max residual, e Å ⁻³	0.95	0.37	0.60	0.62	1.27

^a $R = \sum(|F_o| - |F_c|)/\sum|F_o|$; $R_w = [\sum w(|F_o| - |F_c|)^2/\sum wF_o^2]^{1/2}$; $w = 1/\sigma^2(F_o)$. ^b GOF = $[\sum w(|F_o| - |F_c|)^2/(N_{obs} - N_{parms})]^{1/2}$.

Preparation of [(CpRu*)₂(μ -S)₂Ru(CO)₂(PPh₃)] (**8**).** To a solution of **7·THF** (50.5 mg, 0.0408 mmol) in toluene (10 mL) was bubbled CO for 5 min at room temperature, and the mixture was stirred at 50 °C for 16 h. After removal of the solvent in vacuo, the resultant dark brown solid was recrystallized from benzene–methanol (1 mL/5 mL). The dark brown crystals that formed were filtered off, washed with methanol, and dried in vacuo (12.8 mg, 35%). IR (KBr): 1970, 1921 (s, ν_{CO}). ¹H NMR: δ 7.74–6.97 (m, 15 H, Ph), 1.85 (s, 30 H, C₅-Me₅). ³¹P{¹H} NMR: δ 48.9 (s). Anal. Calcd for C₄₀H₄₅O₂P₂RSu₃: C, 50.25; H, 4.74. Found: C, 50.41; H, 4.90.

X-ray Diffraction Studies. Single crystals suitable for X-ray analyses were sealed in glass capillaries under an inert atmosphere and mounted on a Rigaku AFC7R four-circle diffractometer equipped with a graphite-monochromatized Mo K α source ($\lambda = 0.7107$ Å). Orientation matrixes and unit cell parameters were determined by least-squares treatment of 25 machine-centered reflections with $25^\circ < 2\theta < 40^\circ$. The data collection was performed at room temperature using the ω - 2θ scan technique at a rate of 32 deg min⁻¹ to a maximum 2θ value of 45° (for **4a** and **6·0.5THF**) and 50° (for **5a**, **7·THF**, and **8**). The intensities of three check reflections were monitored every 150 reflections, which showed no significant decay during data collections. Intensity data were corrected for Lorentz–polarization effects and for absorption (ψ scans). Details of crystal and data collection parameters are summarized in Table 3.

Structure solution and refinements were carried out by using the *teXsan* program package.³¹ The heavy atom positions were determined by Patterson methods program (DIRDIF-PATY),³² and the remaining non-hydrogen atoms were found by subsequent Fourier syntheses. All non-hydrogen atoms were refined anisotropically by full-matrix least-squares tech-

niques for **4a**, **5a**, and **7·THF**, while for **6·0.5THF**, the carbon and oxygen atoms in the solvating THF molecule were refined isotropically. For **8**, each of three phenyl rings was placed at the two disordered positions as rigid groups and refined isotropically with a 50% occupancy. The hydrogen atoms of the hydrido ligand in **6·0.5THF** and **7·THF** were found in the final difference Fourier map, while all other hydrogen atoms except those in the solvating THF molecule in **6·0.5THF** were placed at calculated positions. The positional parameters of the hydrogen atoms in the hydrido ligands in **7·THF** were included in the final stages of refinements, whereas all other hydrogen atoms were included with fixed parameters. The atomic scattering factors were taken from ref 33, and anomalous dispersion effects were included; the values of $\Delta f'$ and $\Delta f''$ were taken from ref 34.

Acknowledgment. This work was supported by a Grant-in-Aid for Specially Promoted Research (Grant No. 09102004) from the Ministry of Education, Science, Sports, and Culture of Japan.

Supporting Information Available: Tables of atomic coordinates and equivalent isotropic thermal parameters, anisotropic thermal parameters, and full bond lengths and angles for **4a**, **5a**, **6·0.5THF**, **7·THF**, and **8** (71 pages). Ordering information is given on any current masthead page.

OM980214D

(32) PATTY: Beurskens, P. T.; Admiraal, G.; Beurskens, G.; Bosman, W. P.; Garcia-Granda, S.; Gould, R. O.; Smits, J. M. M.; Smykalla, C. *The DIRDIF program system*; Technical Report of the Crystallography Laboratory: University of Nijmegen, The Netherlands, 1992.

(33) *International Tables for X-ray Crystallography*; Kynoch Press: Birmingham, England, 1974; Vol. IV.

(34) *International Tables for X-ray Crystallography*; Kluwer Academic Publishers: Boston, MA, 1992; Vol. C.

(31) *teXsan: Crystal Structure Analysis Package*; Molecular Structure Corp.: The Woodlands, TX, 1985 and 1992.